Seasonal survey of the composition and degradation state of particulate organic matter in the Rhone River using lipid tracers.

M.-A. Galeron[1], R. Amiraux[1], B. Charriere[2], O. Radakovitch[3], P. Raimbault[1], N. Garcia[1], V. Lagadec[1], F. Vaultier[1], J.-F. Rontani[1]

[1] Aix-Marseille University, Mediterranean Institute of Oceanography (MIO), 13288, Marseille, Cedex 9; Université du Sud Toulon-Var, 83957, CNRS-INSU/IRD UM 110, France.
[2] Centre de Formation et de Recherche sur l'Environnement Méditerranéen (CEFREM, UMR CNRS 5110), Bât. U, Université de Perpignan, Via Domitia (UPVD), 66860 Perpignan, France.
[3] CEREGE UM34, Aix Marseille Université, CNRS, IRD, CDF, 13545 Aix-en-provence

Correspondence to: M.-A. Galeron (marie-aimee.galeron@mio.osupytheas.fr)

Abstract:

Lipid tracers including fatty acids, hydroxyacids, *n*-alkanols, sterols and triterpenoids were used to determine the origin and fate of suspended particulate organic matter (POM) collected in the Rhone River (France). This seasonal survey (April 2011 to May 2013) revealed a year-round strong terrestrial higher-plant contribution to the particulate organic matter (POM), with significant algal inputs observed in March and attributed to phytoplanktonic blooms likely dominated by diatoms. Major terrigenous contributors to our samples are gymnosperms, and more precisely their roots and stems, as evidenced by the presence of high proportions of ω-hydroxydocosanoic acid (a suberin biomarker). The high amounts of coprostanol detected clearly show that the Rhone River is significantly affected by sewage waters.

Specific sterol degradation products were quantified and used to assess the part of biotic and abiotic degradation of POM within the river. Higher-plant-derived organic matter appears to be mainly affected by photo-oxidation and autoxidation (free radical oxidation), while organic matter of mammal or human origin, evidenced by the presence of coprostanol, is clearly more prone to bacterial degradation. Despite the involvement of an intense autoxidation-inducing homolytic cleavage of peroxy bonds, a significant proportion of hydroperoxides is still intact in higher plant debris. These compounds could affect the degradation of terrestrial material by inducing an intense autoxidation upon its arrival at sea.

Key words: Rhône River: Rhone; Particulate organic matter; Lipid tracers; Biotic and abiotic degradation; Autoxidation; Photo-oxidation; Hydroperoxides.

25

26 # 1. Introduction

27 With an average water discharge of 1700 m^3 s^{-1} (Ludwig et al., 2009), the Rhone is the main
28 freshwater contributor to the Mediterranean Sea. Based on various studies, the mean annual flux of
29 suspended matter is about 6.7 x 10^6t yr^{-1} over the period 1967-2008 (Eyrolle et al., 2012), and the
30 annual particulate organic carbon (POC) flux was estimated to be 1.94±1.09 x 10^5 t yr^{-1} (Sempéré et
31 al., 2000). The labile POC fraction, calculated as the carbon contribution from sugars and amino
32 acids to Total POC, was estimated to be between 3 and 27% depending on the amount of SPM
33 (Sempéré et al., 2000). The Rhone River represents 14% and 10% of fresh water and particulate
34 carbon input to the Mediterranean Sea, respectively (Ludwig et al., 2009). Given the importance of
35 such a contribution, it is crucial to study the provenance and composition of the organic matter
36 found in the Rhone, prior to its arrival in the Mediterranean Sea.
37 Up until recently, it was widely considered that the terrestrial particulate organic matter (TPOM)
38 flowing into oceans through rivers was refractory to degradation (biotic and abiotic), since it was
39 constituted of terrestrial plant debris previously degraded during transport (de Leeuw and Largeau,
40 1993; Wakeham and Canuel, 2006). However, coastal sediments have shown very little trace of a
41 terrestrial OM signature (Hedges and Keil, 1995; McKee et al., 2004), which implies that either
42 global carbon fluxes and budgets are wrong, or, and it is more likely, that terrestrial POM
43 undergoes a rapid and intense degradation upon its arrival at sea (Hedges et al., 1997). The belief
44 that terrestrial POM is refractory to all sorts of decomposition has been recently challenged through
45 studies in the Mediterranean Sea (Bourgeois et al., 2011) and Northern Canada (Rontani et al.,
46 2014b), showing that well-preserved TPOM is heavily degraded upon leaving river systems. This is
47 why we intend to study the chemical structure and degradation state of TPOM in the Rhone River,
48 in order to better understand how such an intense degradation can be possible at sea, while it wasn't
49 during freshwater transport.

In comparison with bulk geochemical analyses, where $\delta^{13}C$ terrestrial end-member determination is precarious, $\delta^{13}C$ signatures of organic matter at a molecular level can be more specific (Tolosa et al., 2013). Unfortunately, carbon isotopic data in freshwater ecosystems is not always source-specific, because freshwater phytoplankton and terrestrial plants can often produce similar $\delta^{13}C$ signatures (Cloern et al., 2002). Many studies used biomarkers such as lipids, cutins or waxes in sediment or soil samples in order to determine the specific contribution of plants in organic matter (Amelung et al., 2008; Simpson et al., 2008). Sterols (steroidal alcohols) have specific structural features that can be linked to a restricted number of organisms (Volkman, 1986), and can be used to determine the main contributors to a pool of organic matter. Their degradation products, such as stanols, 3,6-diols, or triols, can also inform on the type of degradation undergone (Christodoulou et al., 2009; Rontani et al., 2009). On the other hand, cuticular waxes and cutins can be linked to relatively specific higher plant groups (Mueller et al., 2012), allowing an estimation of the contribution of terrestrial plants to the OM.

There are no studies dealing with the composition of the plant-derived particulate organic matter carried along the Rhone River in the literature. We propose to confirm the hypothesis according to which the POM sampled in the Rhone is mainly constituted of terrestrially-produced organic matter travelling with the runoff, while also identifying other sources of OM, sometimes significantly aquatic/planktonic. Although limited research has been done on freshwater plankton dynamics in the Rhone, it has been found that phytoplankton communities in the middle Rhone suffer a high turnover (Fruget et al., 2001) implying an important potamoplankton input in the particulate organic matter flowing down the river.

Using specific lipids and their degradation products, here we report for the first time on the different sources of OM in the Rhone River and discuss the main degradation processes affecting this OM.

2. Materials and methods

2.1. Study area and Sampling

The Rhone River is 816 km long and has a drainage area of 97,800 km^2 (Figure 1). The Rhone being a river prone to seasonal flooding, samples span a wide range of water flow conditions in order to be as representative as possible (Figure 2).

To monitor temporal variations of suspended particulate matter (SPM), POC, nutrients and lipidic biomarkers in the Rhone River, 30 surface water and particle samples were collected between April 2011 and May 2013 at the Rhone River reference riverine station of Arles, 40 km upstream from the river mouth (Figure 1).

The high frequency study of the nutrients and particulate matter input by the Rhone to the Mediterranean Sea has been carried out since 2010 in the framework of the national program MOOSE (Mediterranean Ocean Observing System for the Environment). Monitoring was undertaken at the Arles station (Figure 1). Sampling included filtering between 100 and 400 mL of water on GF/F glass fiber filters, as well as particles collection using a high-speed centrifuge device (CEPA Z61) coated with teflon to avoid metal contamination. For suspended matter determination, water samples were filtered on pre-weighted GF/F filters. After drying, filters were weighted to determine the suspended particulate matter (SPM) content (in $mg.l^{-1}$). Non-weighted filters were used to quantify Particulate Organic Carbon (POC) contents: the filters were acidified with 50 - 100µl 0.5N sulfuric acid and dried overnight at 60°c (Raimbault et al., 1999). POC contents were determined using high combustion (900°C) procedure on a CN Integra mass spectrometer (Sercon). Filtrates were used to analyze inorganic nutrients (nitrate, nitrite, phosphate) using the automated colorimetric method described in Aminot and Kérouel (2007), while samples for silicate analysis were filtrated through a 0.45µm polycarbonate membrane and kept at 5°C until analysis. Uncertainty of SPM is estimated to be 0.05 $mg.l^{-1}$ while the analytical error for POC determination is 5 µM (both errors were calculated during method validation, using replicates, and take into

account scale and spectrometer precision and detection limits). Chlorophyll concentration was quantified using methanol extraction according to Raimbault et al. (2004). Samples (filters, filtrates and particles) were immediately frozen at -20°C until analysis.

2.2. Chemical treatment of the samples

Prior to analysis all samples were thawed and their water content was measured through the weighting of humid versus oven-dried particles: Dry particles (g)/Humid particles (g) *100. The suspended particles collected (between 200 and 450 mg per sample) first needed to be reduced with $NaBH_4$ and saponified. $NaBH_4$-reduction of hydroperoxides to alcohols that are amenable to gas chromatography-electron impact mass spectrometry (GC-EIMS) is essential for estimating the importance of photo-oxidative and autoxidative degradation in natural samples (Marchand and Rontani, 2001). Without this preliminary treatment, these labile compounds can be thermally cleaved during alkaline hydrolysis or GC analysis and thus be overlooked during conventional organic geochemical studies. Lipids and their degradation products in the resulting total lipid extracts (TLEs) were then quantified by GC-EIMS. All manipulations were carried out using foil-covered vessels in order to exclude photochemical artifacts. It is well known that metal ions can promote autoxidation during hot saponification (Pokorny, 1987). The prior reduction of hydroperoxides with $NaBH_4$ allowed us to avoid such autoxidation artifacts during the alkaline hydrolysis.

Particles were placed in methanol (MeOH) (15 ml) and hydroperoxides were reduced to the corresponding alcohols with excess $NaBH_4$ (70 mg; 30 min at 20 °C). During this treatment, ketones are also reduced and the possibility of some ester cleavage cannot be excluded.

Saponification was carried out on reduced samples. After $NaBH_4$ reduction, 15 ml water and 2.24 g KOH were added and the mixture directly saponified by refluxing for 2 h. After cooling, the content of the flask was acidified with HCl (pH 1) and extracted (3 x) with dichloromethane (DCM). The

combined DCM extracts were concentrated to give the TLE. After solvent evaporation, residues were taken up in 300 µl of pyridine/N,O-bis(trimethysilyl)trifluoroacetamide (BSTFA; Supelco; 2:1, v:v) and silylated for 1 h at 50 °C to convert OH-containing compounds to TMSi-ether or ester derivatives. After evaporation to dryness under a stream of N_2, the derivatized residues were taken up in 100µL BSTFA (to avoid desilylation of fatty acids) and an appropriate amount of ethyl acetate, depending on the concentration in lipids in each sample, in order to get the best possible GC-EIMS reading. It should be noted that under these conditions steran-3β,5α,6β-triols were silylated only at C3 and C6 and thus need to be analyzed with great care (Rontani et al., 2014b).

A different treatment was used to quantify hydroperoxides and their ketonic and alcoholic degradation products. The samples were extracted three times with chloroform-MeOH-H_2O (1 : 2 : 0.8, v/v/v) using ultrasonication. The supernatant was separated by centrifugation at 3500G for 9 min. To initiate phase separation, purified H_2O was added to the combined extracts to give a final volume ratio of 1 : 1 (v/v). The upper aqueous phase was extracted three times with DCM and the combined DCM extracts were filtered and the solvent removed via rotary evaporation. The residue obtained after extraction was dissolved in 4 ml of DCM and separated in two equal subsamples. After evaporation of the solvent, degradation products were obtained for the first subsample after acetylation (inducing complete conversion of hydroperoxides to the corresponding ketones, Mihara and Tateba, 1986) and saponification and for the second after reduction with $NaBD_4$ and saponification. Comparison of the amounts of alcohols present after acetylation and $NaBD_4$ reduction made it possible to estimate the proportion of hydroperoxides and alcohols present in the samples, while after $NaBD_4$-reduction deuterium labelling allowed to estimate the proportion of ketones really present in the samples (Marchand and Rontani, 2003).

2.3. GC-EIMS analyses

Lipids and their oxidation products were quantified using an Agilent 7850-A gas chromatograph connected to an Agilent 7000-QQQ mass spectrometer. The following conditions were employed:

30 m x 0.25 mm (i.d.) fused silica column coated with HP-5MS (Agilent; film thickness: 0.25 µm); oven programmed from 70 to 130 °C at 20 °C/min, then to 250 °C at 5 °C/min and then to 300 °C at 3 °C/min; carrier gas (He), 1.0 bar; injector (splitless), 250 °C; injector (on column), 50 °C; electron energy, 70 eV; source temperature, 230 °C; quadrupole temperature, 150 °C; m/z 40-700; collision energy, ranging from 5 to 15 eV; collision flow, 1.5 ml/min (N_2); quench flow, 2.25 ml/min (He); cycle time, 0.2 s. An on-column injector was used for the analysis of sterol degradation products and a splitless injector for the analysis of FA degradation products. Compounds were assigned by comparison of retention times and mass spectra with those of standards and quantified (calibration with external single standards) with GC-EIMS. For low concentrations, or in the case of co-elutions, quantification was achieved using selected ion monitoring (SIM) or Multiple Reaction Monitoring (MRM). The main characteristic mass fragment ions used to quantify degradation products of sterols have been described previously (Christodoulou et al., 2009; Rontani et al., 2011). Using replicates, the analytical standard error for lipid quantification (from preparation to integration) was estimated to be 14% (Standard Error = Standard Deviation / √(n) for n replicates).

2. Results and discussion

3.1 Water discharge, Suspended Particulate Matter (SPM) and Particulate Organic Carbon (POC)

Water flow patterns in the Rhone show pronounced seasonal variations predominantly influenced by 3 factors that can induce maximum discharge (Vivian, 1989): snow melting (May-June), intense rains in the south basin (October-November) and rains over the entire basin (January-march). During our sampling period the daily flow rate fluctuated between 680 (19 September 2012) and 4661 $m^3.s^{-1}$ (5 November 2011; Figure 2). Suspended Particulate Matter (SPM) and POC concentrations (Figure 2) ranged from 6.5 to 1381.3 $mg.l^{-1}$ and from 17.9 to 1383.3 µM C, respectively.

178 The temporal evolution of suspended particulate matter (SPM) clearly followed the same pattern
179 than water discharge (Figure 2), which is typical for river systems (Jansson, 1982). The samples
180 collected on flood dates (November 2011, May 2013, liquid discharges above 3000 $m^3.s^{-1}$) display
181 the highest SPM content and POC values (Figure 2). POC expressed as a percentage of SPM,
182 ranged from 0.8 to 11.6%, and tends to be lower when water flows are highest (Sempéré et al.,
183 2000)
184

185 ## 3.2. Use of lipid tracers to estimate the composition and origin of POM
186 ## collected in the Rhone River

187 ### 3.2.1. Sterols

188 Based on a literature review, cholest-5-en-3β-ol (cholesterol), 24-ethylcholest-5-en-3β-ol (sitosterol
189 if the C-24 stereochemistry is 24α), cholesta-5,24-dien-3β-ol (desmosterol), 24-methylcholesta-
190 5,24(28)-dien-3β-ol (24-methylenecholesterol), 24-methylcholesta-5,22-dien-3β-ol (brassicasterol
191 and/or epi-brassicasterol depending on C-24 stereochemistry) and 24-methylcholest-5-en-3β-ol
192 (campesterol) have been selected as tracers of the origin of POM. Apart from cholesterol, which can
193 originate from a wide number of sources, all the other quantified sterols are relatively source-
194 specific. Sitosterol constitutes the major sterol in higher plants, even though it can also be found in
195 diatoms (Volkman, 1986), and is often used to trace terrestrial organic matter in lacustrine and
196 marine systems (e.g. Meyers and Ishiwatari, 1993). Desmosterol is mainly found in algae
197 (Volkman, 1986). 24-Methylenecholesterol is mainly found in diatoms, more particularly in the
198 *Thalassiosira* and *Skeletonema* genera in the marine realm (Volkman, 2003). Epi-brassicasterol is
199 mostly found in algae (Volkman, 1986).
200 All samples are dominated by sitosterol and cholesterol, with proportions being on average three
201 times higher than those of the other sterols, apart from the March 6, 2012 sample (Table 1). This
202 sample exhibits a rather different profile, dominated by desmosterol (0.122 $\mu g.mg^{-1}$ (dry weight))

and 24-methylenecholesterol (0.096 μg.mg^{-1} (dry weight)), with a strong contribution from brassicasterol (0.026 μg.mg^{-1} (dry weight)) compared to all other samples. All these sterols have been considered to be planktonic markers, and have been summed to compose the planktonic sterol fraction shown in Figure 3A. This fraction forms the major part of the total sterol fraction of the March 2012 sample, evidencing a phytoplanktonic bloom event. Given the nature of the sterols involved (desmosterol, methylene-cholesterol), diatoms seem to be major contributors (Rampen et al., 2010). This concurs with the drops in silica observed at the same period (MOOSE data, unpublished). As we see an increase, although less important in the proportion of planktonic sterols in the Spring 2013 samples (20 times less in quantity when compared to the 6 March 2012 sample, but still constituting 31 and 27% of the total of all sterols quantified in the 12 March and 21 March 2013 samples respectively), this type of planktonic event is probably a yearly spring occurrence but our sampling frequency was not adapted to study blooms that can appear and disappear in a matter of days. Sitosterol has been previously identified in marine algae, and more widely as the major sterol in higher terrestrial plants (Volkman, 1986; 2003). However the clear increase observed here in March 2012 demonstrates that it is also present in potamoplankton (Figure 3A). The presence of cholesterol can indicate a zooplankton contribution (Volkman, 1986), but it is also often found in freshwater algae (Volkman et al., 1981; Gagosian et al., 1983), and can also evidence human impacts (Sicre et al., 1993). The relatively high proportions of 5β(H)-cholestan-3β-ol (coprostanol) detected in the samples investigated (see section 3.3.2) clearly show that in the Rhone River cholesterol mainly arises from waste water inputs (Brown and Wade, 1984).

We also looked at the ratio sitosterol/campesterol (Table 1) as an indicator of the terrigenous versus diatom origin of our POM. While many plants have a sitosterol/campesterol ratio of less than 4 (Volkman 1986), Nishimura and Koyama (1977) reported values ranging from 11.5 (*Pinus densiflora*) to 31 (holly *Ilex pedunculosa*). Dachs et al. (1998) identified the threshold of 1 as the limit under which samples are dominated by OM of aquatic origin, and above which sources of OM are terrigenous. In our case, all the samples present a sitosterol/campesterol ratio above 1, mainly

between 2 and 8 (up to 12). Three samples show a ratio near 1 (July 2011 and 2012 and March 2012; Table 1), a low value which confirms the presence of diatoms in the plankton since freshwater diatoms exhibit sitosterol/campesterol ratios close to 1.0 (Ponomarenko et al., 2004).

3.2.2. Terrestrial vascular plant biomarkers

The contribution of terrestrial vascular plants to our samples is also evidenced by the presence of the triterpenoids betulin (lup-20(29)-ene-3β,28-diol), oleanolic (3β-hydroxyolean-12-en-28-oic) and ursolic (3β-hydroxyurs-12-en-28-oic) acids (Razboršek et al., 2008) as well as components of cuticular waxes (16,8-11-dihydroxyhexadecanoic, ω-hydroxyhexadecanoic, ω-hydroxyoleic and 18-hydroxyoctadec-9-enoic acids) (Kolattukudy, 1980) (Figure 3B). Betulin has been proposed as a tracer for paper birch (Fine et al., 2001), a common species along the Rhone River, while oleanolic and ursulic acids are widely distributed in terrestrial higher plants (Liu, 1995). The amount of cuticular waxes is variable amongst samples, between 0.02 and 3.8 $\mu g.mg^{-1}$(dry weight), with the highest in the 5/4/2011, 2/5/2013 and 4/11/2011 samples (3.8, 2.2 and 1.7 $\mu g.mg^{-1}$ respectively). Two of these sample dates (2 May 2013 and 4 November 2011) happen to be flood dates. It is clear that floods, during which higher water flows are coupled to surface runoff, collect and carry more terrestrial plant leaf debris, and hence increase the amount of cuticular waxes found in our samples. The yearly variations in quantity are probably due to the fact that waxes (linear compounds) are more easily degraded by bacteria than cyclic structures such as sterols or triterpenoids (Atlas and Bartha, 1992).

The betulin and sitosterol concentrations are significantly correlated in most of our samples (r=0,67 between sitosterol and betulin, on 29 samples, p-value = 3.10^{-5}, excluding the March, 6, 2012 sample due to its out-of-range phytoplanktonic profile), thus reinforcing the idea that in the Rhone

256 River sitosterol mainly results from terrestrial higher plant inputs. However, at the time of the
257 spring bloom a significant part of this sterol seems to derive from potamoplankton (Figure 3A).
258
259 Another ratio commonly used to attest to the terrigenous origin of compounds is the Terrigenous-to-
260 Aquatic ratio (TAR, Bourbonnière & Meyers, 1996). Here we used the $TAR_{(AL)}$ as calculated by
261 Van Dongen et al. (2008) for *n*-alkanols: $(C_{26}+C_{28})/(C_{16}+C_{18})$. The $TAR_{(AL)}$ in our samples is
262 always above 1, and clearly indicates a strong terrigenous contribution to the suspended particulate
263 matter found in the lower Rhone. The Average Chain Length of *n*-alkanols, a proxy positively
264 correlated to the abundance of higher plant debris (Van Dongen et al., 2008), ranged from 26 to 22
265 across all samples, also attesting to the strong contribution of terrestrial vascular plants. The long-
266 chain even-numbered *n*-alkanol profiles show a strong contribution of C_{22} and C_{28} *n*-alkanols.
267 Compared with those previously described in the literature (Diefendorf et al., 2011), this
268 characteristic suggests a strong gymnosperm contribution, which concurs with the low amounts of
269 long-chain *n*-alkanes detected.
270

271 3.2.3. Chlorophyll

272 The available data on chlorophyll *a* (MOOSE database, only available for 2012 and 2013) shows a
273 content variability between 0.9 (10 October and 6 November, 2012) and 14.0 (3 April 2012) $mg.m^{-3}$
274 (Figure 4A). Chlorophyll *a* is frequently used as a proxy for photosynthetic organisms and the
275 variation observed here is consistent with the hypothesis of a yearly phytoplanktonic spring bloom,
276 with a larger magnitude for the 2012 event.
277

278 3.2.4. Fatty acids

279 A number of saturated linear fatty acids have been found in our samples, with $C_{16:0}$ and $C_{18:0}$ being
280 the most abundant (Table 2). These fatty acids are not specific, and can stem from a number of
281 sources including terrestrial vascular plants, algae and bacteria (Volkman et al., 1981). More

282 recently. $C_{16:1\omega7}$ and $C_{20:5\omega3}$ (eicosapentaenoic acid) were identified as 2 of the main fatty acids in
283 Bacillariophyceae (Taipale et al., 2013). These 2 markers are present in our samples, and together,
284 form 40.5 and 34.1% of the 6 March 2012 and 12 March 2013 samples (versus an average of 13,2%
285 across all samples), which, when coupled with our sterol analysis, concurs with our hypothesis that
286 diatoms are major contributors in the algal blooms identified. It is worth noting that in the 3
287 October 2012 sample, $C_{16:1\omega7}$ forms 53.6% of all quantified fatty acids, while $C_{20:5\omega3}$ is completely
288 absent (0%), and therefore these markers alone cannot be considered to be specific enough in
289 natural river water samples which can contain a number of fatty acids from various sources.
290 Longer-chain saturated fatty acids (between C_{20} and C_{28}) with a strong even-chain predominance,
291 which are specific to the epicuticular waxes of vascular plants (Kunst and Samuels, 2003), are
292 scarcely present in our samples, with C_{20} and C_{22} being the most abundant relative to the others:
293 over 98% (on average) of the total of long-chain (C_{20}-C_{28}) saturated fatty acids across all samples.
294 Due to the high degradability of fatty acids, a number of them could not be quantified, potentially
295 leading to an underestimation of higher plant contribution.
296 Polyunsaturated fatty acids are present in very low proportions in our samples, apart from the
297 06/03/2012 and 12/03/2013 samples where they contributed to 44 and 40% of total fatty acids
298 (Figure 3C - quantified using the total of all PUFA quantified between C_{14} and C_{26}). These high
299 contributions support the presence of a high proportion of fresh algal material in these samples.
300 If we compare the average chain length (ACL) of fatty acids in our samples with that of *n*-alkanols,
301 it appears clearly that the ACL of fatty acids is lower, with an average of 16.7 across samples,
302 against 23.9 for alcohols. It is widely accepted that fatty acids are more prone to bacterial
303 degradation than other lipids (Wakeham, 1995), and long-chain fatty acids tend to be degraded
304 more efficiently by a number of bacteria (Novak and Carlson, 1970). Such a bacterial degradation
305 could explain the ACL difference between *n*-alkanols and fatty acids, and the lack of terrestrial
306 higher-plant fatty acids in our samples, while other markers for higher plants (such as waxes or
307 betulin) are present in large quantities. This is reinforced by the fact that we also find a relatively

high proportion of vaccenic acid in our samples, a specific marker for bacterial activity (Sicre et al., 1988)

3.2.5. Hydroxyacids

Hydroxyacids contents were low during the period studied but some samples (18/07/2011, 4/11/2011 and 16/01/2012) exhibited high amounts of C_{22} ω-hydroxyacid and small quantities of C_{20} and C_{24} homologues (Table 2). These compounds are generally considered to be suberin markers when found in soil (Nierop, 1998; Otto et al., 2005), even though they have been found in leaves and stems of higher plants as well (Mendez-Millan et al., 2010). Suberin is a cell wall component of cork cells, and is mainly found in bark, woody stems, and roots (Kolattukudy, 1980). Given the geographical location of our sampling point, we can consider this compound to be a marker of industrial activity, probably associated to a paper paste mill being implanted less than 3 km upstream. The mill uses mainly local conifers (collected within a 250 km radius according to the company, Paper Excellence (2014)), more particularly *Pinus halepensis*, *Pinus nigra*, and *Pinus sylvestris* (Etude AGRESTE, 2011) and is authorized to reject a certain amount of waste water in the river. This is consistent with our findings that the POM is dominated by gymnosperms. *Pinus* species also display a sitosterol/campesterol ratio comprised between 5 and 10 (Conner et al., 1980) in line with most of our samples as well. This industrial contamination could explain the large contribution of gymnosperms to our POM, and implies that we consider the extra input of terrestrial plant matter that will be released, and degraded, at sea.

As a summary, the overall lipid composition of the Rhone River SPM is characterized by major terrestrial higher plant components (mainly derived from gymnosperms) with episodic, but significant, contributions from freshwater algal material (probably dominated by diatoms) in the spring. Despite the strong concentration of industries along this river, SPM appears to be very

weakly contaminated by petroleum hydrocarbons, but is strongly impacted by the local paper mill and wastewater discharges (see section 3.2.2).

3.3. Use of lipid tracers to estimate the degradation state of POM from the Rhone River

If they can inform us on the origin of organic matter in natural environments, lipid biomarkers are also invaluable in helping us estimate biotic and abiotic alterations of organic matter and determine what are the main processes involved in its degradation. Products resulting from the degradation of sterols, chlorophyll, monounsaturated fatty acids and hydroxyacids are among the most useful and specific tracers.

3.3.1. Chlorophyll

The absorption of light by some compounds, called photosensitizers, in the presence of oxygen (regardless of these compounds being endogenous or not) causes an oxidation whose effects, chemical or biological, are mostly adverse (Spikes and Straight, 1967). Photosensitizers induce chemical reactions via the absorption of light that would not occur in their absence. Photosensitizers (Sens) are involved in indirect photo-oxidative processes: they have 2 systems of electronically excited states, ^{1}Sens and ^{3}Sens. The triplet state is much longer lived than the singlet state, which is the initial product issued from light absorption. Indirect photo-oxidation (photo-sensitized oxidation) can be intense during the senescence of phototrophic organisms (Rontani, 2012) due to the presence of chlorophyll, which is a very efficient photosensitizer (Foote, 1976) capable of generating singlet oxygen particularly reactive towards unsaturated cellular components (Type II photoprocesses). Chlorophyll may be also directly photodegraded by solar light (Nelson, 1993). Direct photodegradation of chlorophyll and Type II photo-oxidation of unsaturated cellular components can be thus considered two competitive photo-processes.

In the photic layer of aquatic environments, photo-oxidation has long been considered a major degradation process for phytoplankton chlorophyll pigments (Lorenzen, 1967; Vernet, 1991). Since we have no marker stable and specific enough for chlorophyll tetrapyrrolic ring photodegradation, we used the CPPI (Chlorophyll Phytyl side chain Photodegradation Index) for the in-situ determination of the rate of photodegradation of chlorophyll (Cuny et al., 1999). Indeed, the photodegradation of the chlorophyll phytyl side chain produces 3-methylidene-7,11,15-trimethylhexadecan-1,2-diol (phytyldiol), specific of Type II chlorophyll photodegradation and widespread in the environment (Cuny and Rontani, 1999). The CPPI, (phytyldiol:phytol molar ratio) can be linked, through a mathematical model, to the global quantity of photodegraded chlorophyll (Cuny et al., 1999),

The photodegradation rate of chlorophyll fluctuates greatly (Figure 4B). The 06/03/2012 and 12/03/2013 samples display very low rates (2.6 and 9.8% respectively), in line with our identification of planktonic blooms in March 2012 and 2013. Such blooms result in an increase of fresh chlorophyll inputs, with intact phytyl side chains, and thus in a decrease of CPPI. The dips in chlorophyll photodegradation rates can help us identify blooms, or at least periods when the input of chlorophyll is higher. The summer 2012 samples (July and September) also display a low photodegradation rate ranging from 8.8 to 13.9% while their amount of planktonic sterols increases slightly.

3.3.2. Δ^5-sterols

Δ^5-sterols possess structural features that can be restricted to a limited number of organisms (Volkman, 1986; 2003). Moreover, biotic and abiotic degradation processes result to specific functionalizations of their cyclic skeleton (De Leeuw and Baas, 1986), which are very useful to estimate the relative importance of these processes (Christodoulou et al., 2009; Rontani et al., 2009). Consequently, degradation products of Δ^5-sterols constitute excellent biomarkers for tracing

385 diagenetic transformations of specific organisms (Mackenzie et al., 1982). Using these tracers to
386 evaluate the relative influence of different degradation processes requires that their removal rate (by
387 further degradation) is comparable to that of the parent Δ^5-sterol. Although each sterol and its
388 degradation products may be potentially totally mineralized by marine bacteria, we assume that they
389 should exhibit similar reactivity towards bacterial degradation. This assumption is based on the fact
390 that aerobic biodegradation of sterols generally involves initial attack on the side chain, which is
391 similar in all the degradation tracers selected to that of the corresponding parent Δ^5-sterol.
392 Moreover, it may be noted that 3β,5α,6β-steratriols, employed for autoxidation estimates are weakly
393 affected by abiotic degradation processes. This is also the case for Δ^4-6α/β -hydroperoxysterols
394 (photooxidation tracers), which are much more stable than Δ^5-7α/β - and Δ^7-5α-hydroperoxysterols
395 (Christodoulou et al., 2009). Indeed, β-scission of the alkoxyl radicals resulting from homolytic
396 cleavage of Δ^5-7-hydroperoxysterols and Δ^6-5-hydroperoxysterols affords secondary and tertiary
397 radicals, respectively, more stable than the primary radical resulting from the cleavage of Δ^4-6-
398 hydroperoxysterols (Christodoulou et al., 2009). Moreover, proton driven cleavage (Hock cleavage)
399 of Δ^5-7-hydroperoxysterols and Δ^6-5-hydroperoxysterols involves a highly favored migration of
400 vinyl group (Frimer, 1979), while only an unfavored migration of alkyl group is possible in the case
401 of Δ^6-5-hydroperoxysterols (Rontani et al., 2014).
402 Aerobic bacterial hydrogenation may convert Δ^5-sterols to 5α(H)-stanols, 5α(H)-stanones and ster-
403 4-en-3-ones (Gagosian et al., 1982; De Leeuw and Baas, 1986; Wakeham, 1989). During the
404 treatment undergone by our samples ($NaBH_4$ reduction), 5α(H)-stanones and ster-4-en-3-ones are
405 respectively converted in 5α(H)-stanols and ster-4-en-3-ols; these compounds hence constitute
406 useful markers of bacterial degradation of sterols. To evaluate the proportion of biological
407 degradation of cholesterol, and to better trace human impacts on the OM found in the Rhone, we
408 also included coprostanol and epicoprostanol in its biodegradation products. Sterol biodegradation
409 percentages were estimated using Eq. (1a) and (1b). Coprostanol (5β(H)-cholestan-3β-ol) is a stanol
410 that arises from the anaerobic microbial degradation of cholesterol in the digestive tracts of higher

land mammals, including man (Martin et al., 1973). Epicoprostanol (5β(H)-cholestan-3α-ol) is not a major sterol in human faeces, but it is often used as an indicator of sewage treatment (McCalley et al., 1981).

Sitosterol biodegradation % = [sitostanol] / [sitosterol] * 100 (1a)

Cholesterol biodegradation % = [cholestanol + coprostanol + epicoprostanol]/ [cholesterol] * 100 (1b)

Free radical autoxidation yields mainly Δ^5-3β-7α/β-hydroperoxides and in smaller quantities 5,6-epoxysterols and 3β,5α,6β-trihydroxysterols. 3β,5α,6β-trihydroxysterols were chosen as tracers of autoxidation (Christodoulou et al., 2009; Rontani et al., 2009) and the sterol autoxidation percentage was estimated using Eq. (2) based on autoxidation rate constants calculated by Morrissey and Kiely (2006).

Sterol autoxidation % = ([3β,5α,6β-trihydroxysterols] * 2.4) / [sitosterol or cholesterol] * 100 (2)

$^1O_2$-mediated photo-oxidation (Type II photoprocesses) yields mainly Δ^6-5α-hydroperoxides and to a lower extent Δ^4-3β-6α/β-hydroperoxides. Δ^6-5α-hydroperoxides are unstable and are converted very easily to the non-specific 7-hydroperoxides, so they were discarded as markers of photo-oxidation. Although produced in lesser amounts, Δ^4-3β-6α/β-hydroperoxides, which are relatively stable and highly specific, have been chosen as tracers of photo-oxidation processes and quantified after $NaBH_4$ reduction to the corresponding diols. The percentage of sterol photo-oxidation was estimated using Eq. (3) (Christodoulou et al., 2009), based on the ratio Δ^4-6α/β-hydroperoxides/Δ^6-5α-hydroperoxides found in biological membranes (0.30) (Korytowski et al., 1992).

Sterol photo-oxidation % = ([Δ^4-3β-6α/β-dihydroxysterols] * (1+0.3)/0.3) / [sitosterol or cholesterol] * 100 (3)

436 Here, values are expressed in proportions relative to the amount of remaining parent sterol in the
437 sample. A total percentage of over 100% hence only means that degradation products were present
438 in larger quantities than their associated parent sterol.
439
440 The results of the evaluation of sitosterol and cholesterol degradation processes are shown in Figure
441 5. The most highly degraded samples sitosterol-wise were the ones from 18/07/2011, 26/06/2012
442 and 22/01/2013. Interestingly, cholesterol degradation shows a completely different trend. When
443 looking at the type of degradation undergone by Δ^5-sterols, it also appears clearly that, if auto- and
444 photo-oxidation processes are the major drivers of sitosterol oxidation, biodegradation is the major
445 player in cholesterol degradation. Hedges and Keil (1995) hinted that sterols associated with waxy
446 higher plant material might not be as prone to enzymatic degradation as other sterols, which would
447 explain why sitosterol is only weakly biodegraded in our samples. Indeed, even though we showed
448 that sitosterol is also produced during spring phytoplanktonic bloom, it is mainly derived from
449 higher plants in most of the samples investigated. The dominance of coprostanol relative to
450 cholestanol attests to a strong contribution of human or animal faeces to the cholesterol present in
451 the Rhone River. Here we used two different ratios in order to better understand of how human
452 activities and waste waters affect the Rhone waters. The first ratio, used to determine if waters are
453 affected by waste water inputs and runoff has been previously used by Writer et al. (1995), and is
454 calculated as follows: coprostanol/(cholesterol+cholestanol). These authors have defined a
455 threshold of 0.06 above which samples are considered affected by wastewater inputs and runoff
456 from pastures and feedlots, and below which they can be considered pristine. The second ratio is the
457 epicoprostanol:coprostanol ratio proposed by Mudge and Seguel (1999), in order to illustrate the
458 level of treatment undergone by wastewaters. The higher the ratio, the more treated the waters are,
459 as epicoprostanol is only present in traces in primary sludge, while it is present in much higher
460 quantities in treated sludge (McCalley et al., 1981). Both ratios are represented in Figure 6 and they
461 show that the Rhone is undeniably affected by wastewaters and, to a much lower extent given the

462 historical land use around the Rhone, pasture runoff. However, we noted that both the ratio and the
463 threshold used are unofficial and in no way are proof of a large-scale contamination or pollution.
464 We only highlight here the non-pristine state of the Rhone waters, which is logical given the level
465 of urbanization along the river. The epicoprostanol:coprostanol ratio also shows fluctuations in the
466 level of treatment of wastewaters, and fluctuates with flow rates and precipitation levels.
467 During senescence, unsaturated higher plant lipids (and notably Δ^5-sterols) may be photodegraded
468 (type II photo-oxidation), with chlorophyll acting as a sensitizer (Rontani et al., 1996). Sitosterol
469 present in higher plant phytodetritus should thus have been intensely photodegraded on land.
470 However, the photo-oxidation rate estimates appeared to be relatively low compared to that of
471 autoxidation and biodegradation (Figure 5A). This is probably due to an intense free-radical-driven
472 breakdown of hydroperoxides produced during photo-oxidation (Rontani et al., 2003). The photo-
473 oxidation percentages displayed here are thus certainly underestimated.
474 The presence of large amounts of 24-ethylcholestan-3β,5α,6β-triol in most of the samples indicates
475 that autoxidation plays an important role in the degradation of sitosterol (Figure 5A). Autoxidation
476 (spontaneous free radical reaction of organic compounds with O_2), which has been largely ignored
477 until now in the environment, seems to play a key role in the degradation of sitosterol (Figure 5A)
478 and thus of higher plant material carried by the Rhone River. This assumption was well supported
479 by the detection of significant proportions of compounds deriving from betulin autoxidation (Data
480 not shown). Recently, it has been demonstrated that autoxidation plays a key role in the degradation
481 of terrestrial (Rontani et al., 2014b) and marine (Rontani et al., 2014a) vascular plant debris in
482 seawater. There is clearly a growing body of evidence suggesting that autoxidation reactions can
483 strongly impact the preservation of particulate organic matter in the environment and should be
484 considered carefully alongside other removal processes such as biodegradation when constructing
485 carbon cycles and evaluating carbon budgets. The lowest autoxidation rates observed in samples
486 from 06/03/2012 and 12/03/2013 may be attributed to the phytoplanktonic bloom events, with high
487 inputs of fresh material. While there is variability in the amount and type of degradation undergone

488 by sterols in the sampled particulate matter, it is evident that sitosterol and cholesterol behave very
489 differently when being degraded.
490
491 ### 3.3.3. Unsaturated fatty acids and cuticular waxes
492 Fatty-acid sensitivity to photo- and autoxidation is intrinsically linked to their number of double
493 bonds (Frankel, 1998), and we will only be looking at unsaturated fatty acids here. Unfortunately,
494 oxidation products of polyunsaturated fatty acids (PUFA) are not stable enough to be used to
495 monitor PUFA degradation. In contrast, photo- and autoxidation products of mono-unsaturated fatty
496 acids (allylic hydroperoxyacids) are much more stable, and can be used (after $NaBH_4$-reduction to
497 the corresponding hydroxyacids) as tracers of the abiotic oxidation processes affecting POM
498 (Marchand and Rontani, 2001). Free-radical-mediated oxidation (autoxidation) processes can be
499 easily discriminated against photo-oxidation processes thanks to the specific *cis* allylic
500 hydroperoxyacids specifically produced by autoxidative processes (Marchand and Rontani, 2001).
501 Samples only displayed small amounts of oxidation products of oleic acid (not quantified), probably
502 due to the fact that unsaturated fatty acids and their degradation products are very labile and easily
503 metabolized by bacteria (Marchand et al., 2005). Despite this degradation, the profiles obtained by
504 GC-MS (exhibiting relatively high proportions of *cis* oxidation products) allowed us to confirm the
505 important role played by autoxidation in the degradation of POM in the Rhone River.
506 Cutin is present in cuticles covering all aerial parts of higher plants. It is constituted of biopolyesters
507 mainly composed of hydroxy fatty acids. Long-chain *n*-alkanoic, ω-hydroxy, dihydroxy, trihydroxy
508 and epoxy-hydroxy acids constitute the major aliphatic monomers (Kolattukudy, 1980). It was
509 previously demonstrated that Type II photooxidation processes act on some unsaturated cutin
510 monomers such as ω-hydroxyoctadec-9-enoic acid (ω-hydroxyoleic acid) during the senescence of
511 higher plants (Rontani et al., 2005). $^1O_2$ reacts with the carbon-carbon double bond, and leads to the
512 formation of a hydroperoxide at each unsaturated carbon. Due to the involvement of allylic
513 rearrangements, Type II photosensitized oxidation of ω-hydroxyoleic acid results (after $NaBH_4$-

reduction of hydroperoxides to the corresponding alcohols) in the formation of isomeric allylic 18,(8-11)-dihydroxyoctadecanoic acids, with a *trans* double bond. These compounds constitute interesting specific tracers of higher plant material photo-oxidation. Autoxidation of this compound was never studied, but by analogy with oleic acid oxidation the autoxidative formation of specific *cis* allylic hydroperoxyacids was expected.

Significant amounts of allylic 18,(8-11)-dihydroxyoleic acid, with *cis* and *trans* double bonds have been effectively detected in some (not all) samples analyzed attesting to the involvement of auto- and photo-oxidation of higher plant material (Galeron & Rontani, unpublished data). The high proportions of *cis* isomers observed confirmed the dominance of autoxidation processes. Some samples (16/1/2012, 26/6/2012 and 18/7/2011) even displayed larger amounts of oxidation products than ω-hydroxyoleic acid, which evidences the importance of degradative processes on this compound. The previously discussed yearly variability in cuticular wax content in our samples (see section 3.2.2 and Fig. 3b) explains some of these results.

3.3.4. Hydroperoxide stability in SPM

It was previously proposed that photochemically-produced hydroperoxides could induce intense autoxidation processes in the marine environment (Rontani et al., 2014a). Hydroperoxides resulting from photo-oxidation processes may undergo: (i) heterolytic cleavage catalyzed by protons (Frimer, 1979) and (ii) homolytic cleavage induced by transition metal ions (Pokorny, 1987) or UVR (Horspool and Armesto, 1992). Homolytic cleavage of hydroperoxides would lead to the formation of alkoxyl radicals, which can then: (i) abstract a hydrogen atom from another molecule to give alcohols, (ii) lose a hydrogen atom to yield ketones, or (iii) undergo β-cleavage reactions affording volatile products. During the $NaBH_4$-reduction, hydroperoxides and ketones were reduced to the corresponding alcohols. The sum of the corresponding hydroperoxides, ketones and alcohols was evaluated under the form of alcohols. Application of a different treatment allowed us to specifically

quantify hydroperoxides, alcohols and ketones (remaining in cuticular waxes, phytol, oleic acid, sitosterol and cholesterol oxidation products) (Figure 7).

Clearly, the proportion of remaining hydroperoxides was highest in the case of sterols, with 49.4 and 31.3% respectively for 3,6- and 3,7-diols of sitosterol, and 51.5 and 33.5% for 3,6- and 3,7-diols of cholesterol, against less than 20% (17.3%) for cutins, 12.0% for oleic acid, and 6.6% for phytol. Standard error was calculated based on all the results obtained (Standard Error = Standard Deviation / √(n) for n samples). These results clearly indicate that despite the involvement of an intense free radical oxidation (autoxidation) inducing homolytic cleavage of peroxy bonds, a significant proportion of hydroperoxides is still intact in POM of the Rhone River. This proportion reaches 10% of the parent residual compound in the case of sitosterol and 5% in the case of cholesterol. Probably due to high compartmentalization effects, preservation of these compounds seems to be enhanced in higher plant debris. It was recently proposed that homolytic cleavage of photochemically-produced hydroperoxides in riverine POM could be catalyzed by some redox-active metal ions released from SPM in the mixing zone of riverine and marine waters (Rontani et al., 2014b). Due to the presence of significant amounts of hydroperoxides in higher plant residues, the involvement of intensive autoxidation of this material in the Rhone estuary is thus likely.

4. Conclusions

Based on a two-year study of the particulate organic matter content of the Rhone River, the main freshwater supplier to the Mediterranean Sea, lipid analyses evidenced a strong contribution from terrestrial vascular plants, most notably gymnosperms. Phytoplanktonic cyclical inputs were also observed and identified as seasonal blooms. The observed amounts of sterols of diatom origin and steep drops in silica observed at the time of the blooms led us to suspect diatoms to be major contributors. Specific compounds like suberin markers, coprostanol and epicoprostanol allowed us to identify anthropic impacts on POM composition (paper mill discharging wastewater and treated waste water discharge).

Using specific lipidic degradation products, we were able to identify for the first time the part that bacterial degradation, autoxidation and photo-oxidation play in organic matter degradation in a Mediterranean river. The study of lipid oxidation products showed that autoxidation, which has been largely underestimated until now in the environment, plays a major role in the degradation of plant-derived organic matter: autoxidation-produced degradation products are nearly half as important as the remaining amount of sitosterol (25% on average across all samples), while biodegradation-produced compounds only represent about a quarter (15% on average across all samples). Photo-oxidation degradation products, although probably underestimated, only stand at 10% (on average across all samples) of the remaining sitosterol amounts. While autoxidation processes appeared to play only a minor role during the degradation of sitosterol in the cold Mackenzie River (Arctic) (Rontani et al., 2014b), it is worth questioning the role that temperature plays in OM degradation, and wondering if it influences one degradation process over the others: do the temperatures found in the Rhone River, warmer than those of the Mackenzie, favor autoxidation? However, the low autoxidation state in the Mackenzie River could also be attributed to the presence of significant proportions of fresh sitosterol-producing phytoplanktonic species (Tolosa et al., 2013). Due to the lack of specificity of this sterol, it is clear that identification of autoxidation products of more specific tracers (such as betulin or amyrins) is absolutely necessary to monitor the degradation of higher plant material in rivers and oceans more precisely.

We also noted that cholesterol offers a very different degradation profile, undergoing little autoxidation, but mainly influenced by biotic degradation processes. Cholesterol is non-specific and can come from a number of sources, which is why it is not used as a tracer of the origin or the general degradation state of POM. However, its bacterial degradation products, including coprostanol and epicoprostanol, are good markers of sewage contamination and sewage treatment, and clearly indicated here that the Rhone waters were affected by wastewaters.

590 Finally, we have shown that even through the degradative processes impacting the TPOM flowing
591 down the Rhone, there is still an important quantity of hydroperoxides remaining in the OM, which
592 in turn should favor autoxidation upon the OM arrival at sea.
593

Acknowledgements: This work is a contribution to the Labex OT-Med (n° ANR-11-LABX-0061) funded by the French Government «Investissements d'Avenir» program of the French National Research Agency (ANR) through the A*MIDEX project (n° ANR-11-IDEX-0001-02). It was also supported by the LEFE-CYBER (Les Enveloppes Fluides et l'Environnement) national program, as part of the MORTIMER (Matière ORganique Terrestre rejetée par les fleuves et les rIvières en MER) research program. It was undergone as part of the transversal research axis DEBAT of the Mediterranean Institute of Oceanography, Marseille, France.

Additional data provided by "MOOSE" (Mediterranean Oceanic Observing System for the Environment) with the support of the "Agence de l'Eau Rhone-Méditerranée-Corse". Special thanks to Michel Fornier for providing samples

AGRESTE. En Provence-Alpes-Côte d'Azur, la forêt est sous-exploitée (Rapport du Ministère de l'agriculture, de l'alimentation, de la pêche, de la ruralité et de l'aménagement du territoire), 2011.

Amelung, W., Brodowski, S., Sandhage-Hofmann, A., and Bol, R.. Chapter 6 Combining Biomarker with Stable Isotope Analyses for Assessing the Transformation and Turnover of Soil Organic Matter. In Advances in Agronomy, Donald L. Sparks, ed. (Academic Press), pp. 155–250, 2008.

Aminot, A., and Kérouel, R. Dosage automatique des nutriments dans les eaux marines: méthodes en flux continu (Editions Quae), 2007.

Atlas, R.M., and Bartha, R. Hydrocarbon Biodegradation and Oil Spill Bioremediation. In Advances in Microbial Ecology, K.C. Marshall, ed. (Springer US), pp. 287–338, 1992.

Bourbonniere, R.A., and Meyers, P.A. Sedimentary geolipid records of historical changes in the watersheds and productivities of Lakes Ontario and Erie. Limnology and Oceanography *41*, 352–359, 1996.

Bourgeois, S., Pruski, A.M., Sun, M.-Y., Buscail, R., Lantoine, F., Vétion, G., Rivière, B., and Charles, F. Distribution and lability of land-derived organic matter in the surface sediments of the Rhône prodelta and the adjacent shelf (Mediterranean sea, France): a multi proxy study. Biogeosciences Discussions *8*, 2011.

Brown, R.C., and Wade, T.L. Sedimentary coprostanol and hydrocarbon distribution adjacent to a sewage outfall. Water Research *18*, 621–632, 1984.

Cloern, J.E., Canuel, E.A., and Harris, D. Stable carbon and nitrogen isotope composition of aquatic and terrestrial plants of the San Francisco Bay estuarine system. Limnology and Oceanography *47*, 713–729, 2002.

Christodoulou, S., Marty, J.-C., Miquel, J.-C., Volkman, J.K., and Rontani, J.-F. Use of lipids and their degradation products as biomarkers for carbon cycling in the northwestern Mediterranean Sea. Marine Chemistry *113*, 25–40, 2009.

Conner, A.H., Nagasampagi, B.A., and Rowe, J.W. Terpenoid and other extractives of western white pine bark. Phytochemistry *19*, 1121–1131, 1980.

Cuny P. and Rontani J-F. On the widespread occurrence of 3-methylidene-7,11,15-trimethylhexadecan-1,2-diol in the marine environment : a specific isoprenoid marker of chlorophyll photodegradation. Marine Chemistry *65*, 155-165, 1999.

Cuny, P., Romano, J.-C., Beker, B., and Rontani, J.-F. Comparison of the photodegradation rates of chlorophyll chlorin ring and phytol side chain in phytodetritus: is the phytyldiol versus phytol ratio (CPPI) a new biogeochemical index? Journal of Experimental Marine Biology and Ecology *237*, 271–290, 1999.

Dachs, J., Bayona, J.M., Fowler, S.W., Miquel, J.-C., and Albaigés, J. Evidence for cyanobacterial inputs and heterotrophic alteration of lipids in sinking particles in the Alboran Sea (SW Mediterranean). Marine Chemistry *60*, 189–201, 1998.

De Leeuw, J.W., and Baas, M. Early-stage diagenesis of steroids. Methods in Geochemistry and Geophysics *24*, 101–123, 1986.

De Leeuw, J.W., and Largeau, C. A Review of Macromolecular Organic Compounds That Comprise Living Organisms and Their Role in Kerogen, Coal, and Petroleum Formation. In Organic Geochemistry, M.H. Engel, and S.A. Macko, eds. (Springer US), pp. 23–72, 1993.

Diefendorf, A.F., Freeman, K.H., Wing, S.L., and Graham, H.V. Production of n-alkyl lipids in living plants and implications for the geologic past. Geochimica et Cosmochimica Acta *75*, 7472–7485, 2011.

Eyrolle, F., Radakovitch, O., Raimbault, P., Charmasson, S., Antonelli, C., Ferrand, E., Aubert, D., Raccasi, G., Jacquet, S., and Gurriaran, R. Consequences of hydrological events on the delivery of suspended sediment and associated radionuclides from the Rhône River to the Mediterranean Sea. J Soils Sediments *12*, 1479–1495, 2012.

Fine, P.M., Cass, G.R., and Simoneit, B.R.T. Chemical Characterization of Fine Particle Emissions from Fireplace Combustion of Woods Grown in the Northeastern United States. Environ. Sci. Technol. *35*, 2665–2675, 2001.

Foote, C.S. Photosensitized oxidation and singlet oxygen: consequences in biological systems. Free Radicals in Biology *2*, 85–133, 1976.

Frankel, E.N. Lipid oxidation. The Oily, Dundee, Scotland 129–160, 1998.

Frimer, A.A. The reaction of singlet oxygen with olefins: the question of mechanism. Chem. Rev. *79*, 359–387, 1979.

Fruget, J.-F., Centofanti, M., Dessaix, J., Olivier, J.-M., Druart, J.-C., and Martinez, P.-J. Temporal and spatial dynamics in large rivers: example of a long-term monitoring of the middle Rhone River. Annales de Limnologie - International Journal of Limnology *37*, 237–251, 2001.

Gagosian, R.B., Zafiriou, O.C., Peltzer, E.T., and Alford, J.B. Lipids in aerosols from the tropical North Pacific: Temporal variability. J. Geophys. Res. *87*, 11133–11144, 1982.

Gagosian, R.B., Nigrelli, G.E., and Volkman, J.K. Vertical Transport and Transformation of Biogenic Organic Compounds from a Sediment Trap Experiment Off the Coast of Peru. In Coastal Upwelling Its Sediment Record, E. Suess, and J. Thiede, eds. (Springer US), pp. 241–272, 1983.

Hedges, J.I., and Keil, R.G. Sedimentary organic matter preservation: an assessment and speculative synthesis. Marine Chemistry *49*, 81–115, 1995.

Hedges, J.I., Keil, R.G., and Benner, R. What happens to terrestrial organic matter in the ocean? Organic Geochemistry *27*, 195–212, 1997.

Horspool, W., and Armesto, D. Organic Photochemistry: A comprehensive treatment (Ellis Horwood). 1992.

Jansson, M.B. Land erosion by water in different climates. UNGI Rapport (Sweden), 1982.

Kolattukudy, P.E. Cutin, suberin, and waxes. Biochemistry of Plants: A Comprehensive Treatise, 1980.

Korytowski, W., Bachowski, G.J., Girotti, A.W. Photoperoxidation of cholesterol in homogeneous solution, isolated membranes, and cells: comparison of the 5α, and 6β- hydroperoxides as indicators of singlet oxygen intermediacy. Photochemistry and Photobiology 56, 1-8, 1992.

Kunst, L., and Samuels, A.L. Biosynthesis and secretion of plant cuticular wax. Progress in Lipid Research *42*, 51–80, 2003.

Liu, J. Pharmacology of oleanolic acid and ursolic acid. Journal of Ethnopharmacology *49*, 57–68, 1995.

Lorenzen, C.J. Vertical distribution of chlorophyll and phaeo-pigments : Baja California. Deep Sea Research and Oceanographic Abstracts *14*, 735–745, 1967.

Ludwig, W., Dumont, E., Meybeck, M., and Heussner, S. River discharges of water and nutrients to the Mediterranean and Black Sea: Major drivers for ecosystem changes during past and future decades? Progress in Oceanography *80*, 199–217, 2009.

Mackenzie, A.S., Brassell, S.C., Eglinton, G., and Maxwell, J.R. Chemical fossils: the geological fate of steroids. Science *217*, 491–504, 1982.

Marchand, D., and Rontani, J.-F. Characterisation of photo-oxidation and autoxidation products of phytoplanktonic monounsaturated fatty acids in marine particulate matter and recent sediments. Organic Geochemistry *32*, 287–304, 2001.

Marchand, D., and Rontani, J.-F. Visible light-induced oxidation of lipid components of purple sulfur bacteria: a significant process in microbial mats. Organic Geochemistry *34*, 61–79, 2003.

Marchand, D., Marty, J.-C., Miquel, J.-C., and Rontani, J.-F. Lipids and their oxidation products as biomarkers for carbon cycling in the northwestern Mediterranean Sea: results from a sediment trap study. Marine Chemistry *95*, 129–147, 2005.

Martin, W.J., Subbiah, M.T.R., Kottke, B.A., Birk, C.C., and Naylor, M.C. Nature of fecal sterols and intestinal bacterial flora. Lipids *8*, 208–215, 1973.

McCalley, D.V., Cooke, M., and Nickless, G. Effect of sewage treatment on faecal sterols. Water Research *15*, 1019–1025, 1981.

McKee, B.A., Aller, R.C., Allison, M.A., Bianchi, T.S., and Kineke, G.C. Transport and transformation of dissolved and particulate materials on continental margins influenced by major rivers: benthic boundary layer and seabed processes. Continental Shelf Research *24*, 899–926, 2004.

Mendez-Millan, M., Dignac, M.-F., Rumpel, C., Rasse, D.P., and Derenne, S. Dynamics of shoot vs. root C assessed by natural 13C abundance of their biomarkers. In EGU General Assembly Conference Abstracts, p. 9968, 2010.

Meyers, P.A., and Ishiwatari, R. Lacustrine organic geochemistry—an overview of indicators of organic matter sources and diagenesis in lake sediments. Organic Geochemistry *20*, 867–900, 1993.

Mihara, S., and Tateba, H. Photosensitized oxygenation reactions of phytol and its derivatives. The Journal of Organic Chemistry *51*, 1142–1144, 1986.

Morrissey, P.A., and Kiely, M. Oxysterols: Formation and Biological Function. In Advanced Dairy Chemistry Volume 2 Lipids, P.F. Fox, and P.L.H. McSweeney, eds. (Springer US), pp. 641–674, 2006.

Mudge, S.M., and Seguel, C.G. Organic Contamination of San Vicente Bay, Chile. Marine Pollution Bulletin *38*, 1011–1021, 1999.

Mueller, K.E., Polissar, P.J., Oleksyn, J., and Freeman, K.H. Differentiating temperate tree species and their organs using lipid biomarkers in leaves, roots and soil. Organic Geochemistry *52*, 130–141, 2012.

Nelson, J.R. Rates and possible mechanism of light-dependent degradation of pigments in detritus derived from phytoplankton. Journal of Marine Research *51*, 155–179, 1993.

Nierop, K.G.J. Origin of aliphatic compounds in a forest soil. Organic Geochemistry *29*, 1009–1016, 1998.

Nishimura, M., and Koyama, T. The occurrence of stanols in various living organisms and the behavior of sterols in contemporary sediments. Geochimica et Cosmochimica Acta *41*, 379–385, 1977.

Novak, J.T., and Carlson, D.A. The Kinetics of Anaerobic Long Chain Fatty Acid Degradation. Journal (Water Pollution Control Federation) *42*, 1932–1943, 1970.

Otto, A., Shunthirasingham, C., and Simpson, M.J. A comparison of plant and microbial biomarkers in grassland soils from the Prairie Ecozone of Canada. Organic Geochemistry *36*, 425–448, 2005.

Paper Excellence – Fibre Excellence Tarascon. http://www.paperexcellence.com/mills/fibre-excellence-tarascon/ (April 14, 2014)

Pokorny, J. Major factors affecting the autoxidation of lipids. Autoxidation of Unsaturated Lipids 141–206, 1987.

Ponomarenko, L.P., Stonik, I.V., Aizdaicher, N.A., Orlova, T.Y., Popovskaya, G.I., Pomazkina, G.V., and Stonik, V.A. Sterols of marine microalgae Pyramimonas cf. cordata (Prasinophyta), Attheya ussurensis sp. nov. (Bacillariophyta) and a spring diatom bloom from Lake Baikal. Comparative Biochemistry and Physiology Part B: Biochemistry and Molecular Biology *138*, 65–70, 2004.

Raimbault P., Diaz F., Boudjellal B. Simultaneous determination of particulate forms of carbon, nitrogen and phosphorus collected on filters using a semi-automatic wet-oxidation procedure. Mar. Ecol. Progr. Ser., 180: 289-295, 1999

Raimbault, P., Lantoine, F., and Neveux, J. Dosage rapide de la chlorophylle *a* et des phéopigments a par fluorimétrie après extraction au méthanol. Comparaison avec la méthode classique d'extraction à l'acétone. Océanis *30 (2)*, 189–205, 2004.

Rampen, S.W., Abbas, B.A., Schouten, S., and Damsté, J.S.S. A comprehensive study of sterols in marine diatoms (Bacillariophyta): Implications for their use as tracers for diatom productivity. Limnology and Oceanography *55*, 91, 2010.

Razboršek, M.I., Vončina, D.B., Doleček, V., and Vončina, E. Determination of Oleanolic, Betulinic and Ursolic Acid in Lamiaceae and Mass Spectral Fragmentation of Their Trimethylsilylated Derivatives. Chroma *67*, 433–440, 2008.

Rontani, J.-F. Photo-and free radical-mediated oxidation of lipid components during the senescence of phototrophic organisms. Senescence, Intech, Rijeka 3–31, 2012.

Rontani, J.-F., Cuny, P., and Grossi, V. Photodegradation of chlorophyll phytyl chain in senescent leaves of higher plants. Phytochemistry *42*, 347–351, 1996.

Rontani, J.-F., Rabourdin, A., Marchand, D., and Aubert, C. Photochemical oxidation and autoxidation of chlorophyll phytyl side chain in senescent phytoplanktonic cells: Potential sources of several acyclic isoprenoid compounds in the marine environment. Lipids *38*, 241–254, 2003.

Rontani, J.-F., Rabourdin, A., Pinot, F., Kandel, S., and Aubert, C. Visible light-induced oxidation of unsaturated components of cutins: a significant process during the senescence of higher plants. Phytochemistry *66*, 313–321, 2005.

Rontani, J.-F., Zabeti, N., and Wakeham, S.G. The fate of marine lipids: Biotic vs. abiotic degradation of particulate sterols and alkenones in the Northwestern Mediterranean Sea. Marine Chemistry *113*, 9–18, 2009.

Rontani, J.-F., Zabeti, N., and Wakeham, S.G. Degradation of particulate organic matter in the equatorial Pacific Ocean: Biotic or abiotic? Limnology and Oceanography *56*, 333–349, 2011.

Rontani, J.-F., Vaultier, F., and Bonin, P. Biotic and abiotic degradation of marine and terrestrial higher plant material in intertidal surface sediments from Arcachon Bay (France): A lipid approach. Marine Chemistry *158*, 69–79, 2014a.

Rontani, J.-F., Charriere, B., Sempéré, R., Doxaran, D., Vaultier, F., Vonk, J.E., and Volkman, J.K. Degradation of sterols and terrigenous organic matter in waters of the Mackenzie Shelf, Canadian Arctic. Organic Geochemistry. In press, 2014b.

Sempéré, R., Charrière, B., Van Wambeke, F., and Cauwet, G. Carbon inputs of the Rhône River to the Mediterranean Sea: Biogeochemical implications. Global Biogeochem. Cycles *14*, 669–681, 2000.

Sicre, M.-A., Paillasseur, J.-L., Marty, J.-C., and Saliot, A. Characterization of seawater samples using chemometric methods applied to biomarker fatty acids. Organic Geochemistry *12*, 281–288, 1988.

Sicre, M.-A., Tian, R.C., Broyelle, I., and Saliot, A. Aquatic distribution of 4-desmethyl sterols in the Chang Jiang Estuary, China. Marine Chemistry *42*, 11–24, 1993.

Simpson, M.J., Otto, A., and Feng, X. Comparison of solid-state carbon-13 nuclear magnetic resonance and organic matter biomarkers for assessing soil organic matter degradation. Soil Science Society of America Journal *72*, 268–276, 2008.

Spikes, J.D., and Straight, R. Sensitized Photochemical Processes in Biological Systems. Annual Review of Physical Chemistry *18*, 409–436, 1967.

Taipale, S., Strandberg, U., Peltomaa, E., Galloway, A.W.E., Ojala, A., and Brett, M.T. Fatty acid composition as biomarkers of freshwater microalgae: analysis of 37 strains of microalgae in 22 genera and in seven classes. Aquatic Microbial Ecology *71*, 165–178, 2013.

Tolosa, I., Fiorini, S., Gasser, B., Martín, J., and Miquel, J.C. Carbon sources in suspended particles and surface sediments from the Beaufort Sea revealed by molecular lipid biomarkers and compound-specific isotope analysis. Biogeosciences *10*, 2013.

Van Dongen, B.E., Zencak, Z., and Gustafsson, Ö. Differential transport and degradation of bulk organic carbon and specific terrestrial biomarkers in the surface waters of a sub-arctic brackish bay mixing zone. Marine Chemistry *112*, 203–214, 2008.

Vernet, M. Phytoplankton dynamics in the Barents Sea estimated from chlorophyll budget models. Polar Research *10*, 129–146, 1991.

Vivian, H. Hydrological changes of the Rhône River. Historical Change of Large Alluvial Rivers: Western Europe. John Wiley & Sons New York. P 57-77, 1989.

Volkman, J.K. A review of sterol markers for marine and terrigenous organic matter. Organic Geochemistry *9*, 83–99, 1986.

Volkman, J.K.. Sterols in microorganisms. Appl Microbiol Biotechnol *60*, 495–506, 2003.

Volkman, J.K., Smith, D.J., Eglinton, G., Forsberg, T.E.V., and Corner, E.D.S. Sterol and fatty acid composition of four marine haptophycean algae. Journal of the Marine Biological Association of the United Kingdom *61*, 509–527, 1981.

Wakeham, S.G. Reduction of stenols to stanols in particulate matter at oxic–anoxic boundaries in sea water. Nature *342*, 787–790, 1989.

Wakeham, S.G. Lipid biomarkers for heterotrophic alteration of suspended particulate organic matter in oxygenated and anoxic water columns of the ocean. Deep Sea Research Part I: Oceanographic Research Papers *42*, 1749–1771, 1995.

Wakeham, S.G., and Canuel, E.A. Degradation and Preservation of Organic Matter in Marine Sediments. In Marine Organic Matter: Biomarkers, Isotopes and DNA, J.K. Volkman, ed. (Springer Berlin Heidelberg), pp. 295–321, 2006.

Writer, J.H., Leenheer, J.A., Barber, L.B., Amy, G.L., and Chapra, S.C. Sewage contamination in the upper Mississippi River as measured by the fecal sterol, coprostanol. Water Research *29*, 1427–1436, 1995

Figure Captions

- Figure 1. Rhone River mouth area and sampling location: “Arles”. gR and pR mean grand Rhone and petit Rhone which are the two arms of the river.

- Figure 2: Water Flow ($m^3.s^{-1}$), Suspended Particulate Matter ($mg.l^{-1}$) and Particulate Organic Carbon (POC, μM) of Rhone waters on our sampling dates (MOOSE data). Samples span a wide range of water flow conditions.

- Figure 3: Sitosterol and planktonic sterols (A), cuticular waxes and betulin (B), and Poly-Unsaturated Fatty Acid (PUFA) (C) contents of the different samples. Standard error shown was estimated to be 14% (see section 2.3). Phytoplanktonic blooms are evidenced by the spike in planktonic sterols, and while the other tracers show the terrigenous origin of the POM sampled, the ubiquitous nature of sitosterol is made clear.

- Figure 4: Chlorophyll a levels (MOOSE data) and percentage of photodegradation of chlorophyll (calculated using CPPI (Cuny et al., 1999) in the Rhone waters on and around sample dates

- Figure 5: Biotic and abiotic degradation of sitosterol (A) and cholesterol (B) in the different samples. Full error shown here incorporates the 14% analytical standard error estimated for lipid quantification for all terms of the equations used. Sitosterol and cholesterol clearly have very different degradation patterns.

- Figure 6: Coprostanol:(cholesterol+cholestanol) and epicoprostanol:coprostanol ratios of the different samples. Full error shown here incorporates the 14% analytical standard error estimated for lipid quantification for all terms of the ratios. Contamination threshold is 0.06 (See section 3.3.2).

- Figure 7: Relative percentages of intact hydroperoxides and their ketonic and alcoholic degradation products measured in the case of ω-hydroxyoleic (cuticular waxes) and oleic acids, phytol, sitosterol and cholesterol oxidation products. Standard error was calculated based on the results obtained for all samples.

Table 1: Percentages of sterols (relative to the sum of sterols quantified), and sitosterol:campesterol ratio in the samples investigated.

Date	Sitosterol	Cholesterol	Desmosterol	Brassicasterol	Methylene-Cholesterol	Campesterol	Sitosterol:Campesterol ratio
5 April 2011	74.4	12.7	0.4	4.9	1.2	6.4	11.6
18 July 2011	21.2	45.5	2.6	16.1	3.3	11.3	1.9
4 November 2011	54.1	23.8	1.9	10.0	2.2	8.0	6.7
5 November 2011	60.2	21.4	1.2	7.7	1.7	7.9	7.6
7 November 2011	56.7	28.6	0.4	6.1	1.3	6.9	8.2
14 November 2011	34.6	45.7	0.9	10.0	1.5	7.4	4.7
19 December 2011	52.5	29.1	0.5	7.5	1.9	8.5	6.2
16 January 2012	39.2	43.6	1.3	6.7	1.8	7.4	5.3
6 March 2012	17.6	12.4	28.8	6.2	22.6	12.4	1.4
17 April 2012	36.5	39.3	4.7	8.2	2.9	8.4	4.4
2 May 2012	38.4	41.4	2.1	9.5	1.9	6.7	5.7
22 May 2012	32.5	43.6	4.4	10.3	2.6	6.5	5.0
11 June 2012	35.0	43.5	2.5	9.6	1.6	7.7	4.5
26 June 2012	24.7	54.9	2.6	10.0	1.8	6.0	4.1
25 July 2012	21.6	37.5	3.9	20.8	4.4	11.7	1.8
5 September 2012	22.6	46.6	3.4	15.4	3.3	8.6	2.6
19 September 2012	21.1	44.3	3.8	19.1	3.0	8.7	2.4
3 October 2012	27.4	46.7	2.3	11.9	1.9	9.8	2.8
16 October 2012	42.9	38.9	1.4	7.8	1.4	7.6	5.7
6 November 2012	44.9	36.9	2.0	7.3	1.8	7.1	6.3
17 December 2012	66.3	22.8	1.0	3.5	1.2	5.2	12.7
10 January 2013	46.9	34.8	2.5	7.1	1.5	7.2	6.5
22 January 2013	36.0	48.4	1.4	6.9	1.3	6.1	5.9
4 February 2013	50.0	39.2	0.8	4.0	0.8	5.1	9.8
13 February 2013	55.4	30.7	2.0	4.8	1.3	5.9	9.4
12 March 2013	35.1	27.6	14.5	9.0	7.6	6.2	5.7
21 March 2013	37.4	29.0	11.1	8.9	6.6	7.2	5.2
17 April 2013	35.6	45.6	2.6	7.0	2.5	6.7	5.3
2 May 2013	59.0	24.5	1.1	6.8	1.7	6.8	8.7
13 May 2013	49.7	38.6	0.0	4.6	1.1	6.1	8.2
Average	41.0	35.9	3.6	8.9	3.0	7.6	5.9
Standard deviation	14.6	10.7	5.6	4.2	4.0	1.8	2.8

Table 2: Fatty and Hydroxy Acid (FA/HA) content of the different samples (% of total quantified FA/HA) (PUFA: Poly-Unsaturated Fatty Acids)*double bond position undetermined

	2011							2012														2013								
	5/4	18/7	4/11	5/11	7/11	14/11	19/12	16/1	6/3	17/4	2/5	22/5	11/6	26/6	25/7	5/9	19/9	3/10	16/10	6/11	17/12	10/1	22/1	4/2	13/2	12/3	21/3	17/4	2/5	13/5
$C_{14:0}$	4.4	8.4	5.4	3.5	1.6	4.2	5.1	6.1	11.4	6.8	2.9	2.2	3.8	6.0	2.2	8.2	1.6	1.2	1.5	1.2	1.1	3.9	2.0	1.3	2.1	3.5	5.3	3.6	1.6	4.6
$C_{15:0}$	2.6	2.1	2.1	2.7	1.0	2.1	1.9	2.0	0.4	2.2	2.1	1.1	2.1	2.3	1.1	1.3	0.9	0.9	1.3	1.0	1.0	1.9	2.3	1.1	1.5	0.7	0.8	1.7	1.2	2.5
$C_{15:1}$	0.0	0.0	0.0	0.0	0.0	0.6	0.0	0.0	0.1	0.0	0.0	0.0	0.3	0.0	0.0	0.0	0.0	0.0	0.0	0.0	0.0	0.0	0.0	0.0	0.0	0.0	0.1	0.0	0.0	0.0
Iso-$C_{15:0}$	2.1	4.3	2.8	1.6	0.2	3.2	2.3	3.1	0.1	1.5	1.2	0.4	1.4	1.1	0.7	2.9	0.5	0.9	0.9	0.3	0.2	1.5	0.3	0.2	0.4	0.2	0.5	1.2	0.7	0.5
Anté-iso-$C_{15:0}$	1.4	2.1	2.1	1.3	0.2	2.1	2.3	2.9	0.1	1.3	1.0	0.5	1.2	0.9	0.4	1.4	0.4	0.7	0.9	0.4	0.2	1.5	0.4	0.2	0.5	0.2	0.5	1.1	0.6	0.7
$C_{16:0}$	40.7	42.9	42.6	57.3	40.4	47.2	42.2	46.0	17.9	46.5	58.7	45.3	56.5	64.3	46.2	46.5	46.1	4.8	5.1	50.3	51.8	45.3	63.9	53.7	51.9	25.5	27.2	40.5	54.8	71.0
$C_{16:1\ \omega7}$	5.5	14.6	12.3	5.7	1.2	14.0	7.6	10.7	23.2	11.9	7.0	6.3	5.2	7.0	11.4	12.9	8.5	53.6	6.6	2.4	1.0	6.9	3.8	2.6	3.9	14.1	13.6	8.8	4.1	2.3
$C_{16:2*}$	0.0	0.0	0.0	0.0	0.0	0.0	0.0	0.0	6.1	0.0	0.0	0.0	0.0	0.0	2.4	2.7	0.0	0.0	0.0	0.0	0.0	0.0	0.0	0.0	0.0	0.0	3.2	0.8	0.0	0.0
$C_{16:3*}$	0.0	0.4	0.0	0.0	0.0	0.0	0.0	0.0	11.7	0.0	0.0	0.0	0.0	0.0	0.0	2.8	0.0	0.0	0.0	0.0	0.0	0.0	0.0	0.0	0.0	7.9	6.0	1.2	0.0	0.0
$C_{16:4*}$	0.0	0.0	0.0	0.0	0.0	0.0	0.0	0.0	4.1	0.5	0.0	0.0	0.0	0.0	0.0	0.0	0.0	0.0	0.0	0.0	0.0	0.0	0.0	0.0	0.0	4.5	3.0	0.0	0.0	0.0
$C_{17:0}$	0.9	1.0	0.8	0.9	0.9	1.0	0.7	0.7	0.0	0.6	0.6	0.7	0.7	0.8	0.8	0.6	0.7	1.4	1.2	0.9	0.7	0.8	0.8	0.8	0.6	0.3	0.3	0.9	0.0	0.0
$C_{18:0}$	9.3	9.1	7.5	12.4	20.6	11.0	10.2	12.2	1.2	10.5	13.5	20.3	14.6	13.5	10.7	6.9	12.8	15.3	21.1	24.3	20.5	16.5	16.7	21.3	17.7	5.6	7.3	13.2	18.6	13.2
$C_{18:1\omega9}$ (Oleic)	8.1	6.6	10.6	0.8	6.9	6.3	9.1	8.2	0.9	7.9	6.2	9.5	5.2	0.7	11.8	6.5	14.0	10.0	11.7	9.8	6.4	2.5	4.9	12.3	13.1	7.5	9.0	11.9	10.8	3.5
$C_{18:1\omega7}$ (Vaccenic)	3.3	4.9	4.6	3.7	5.1	5.3	5.7	4.2	0.0	3.6	3.5	6.2	3.5	2.1	6.4	3.2	6.5	7.2	10.1	5.1	2.3	10.5	1.8	3.4	3.9	2.0	3.2	4.8	3.4	0.9
$C_{18:2\omega6}$	3.3	1.2	4.0	0.1	1.5	1.2	3.4	1.7	0.0	2.2	0.9	2.1	0.9	0.0	2.2	1.0	2.8	2.1	2.3	1.9	11.4	4.5	0.9	1.6	2.4	1.9	2.7	2.5	0.0	0.0
$C_{18:3\omega3}$	0.0	0.0	0.0	0.0	0.0	0.0	0.0	0.0	0.0	1.7	0.0	0.0	0.0	0.0	0.0	0.0	0.0	0.0	0.0	0.0	0.0	0.0	0.0	0.0	0.0	0.0	0.0	0.0	0.0	0.0
$C_{18:4\omega3}$	0.0	0.0	0.0	0.0	0.0	0.0	0.0	0.0	5.5	0.0	0.0	0.0	0.0	0.0	0.0	0.0	0.0	0.0	0.0	0.0	0.0	0.0	0.0	0.0	0.0	5.4	3.6	0.0	0.0	0.0
$C_{20:0}$	2.2	0.9	2.0	1.4	3.6	0.9	1.6	1.8	0.1	0.9	1.1	1.6	1.2	0.0	0.8	0.5	1.1	1.3	33.1	1.7	1.7	1.6	0.9	0.7	1.0	0.4	0.7	1.6	1.6	0.4
$C_{20:5\omega3}$	12.2	0.6	0.8	7.0	11.7	0.1	4.4	0.0	17.3	0.9	0.0	2.0	1.7	0.4	2.1	1.3	2.8	0.0	0.0	0.0	0.0	0.0	0.0	0.0	0.0	20.0	12.1	3.9	0.0	0.0
$C_{22:0}$	3.0	0.8	2.0	1.3	3.9	0.8	2.1	0.2	0.0	0.6	1.0	1.4	1.3	0.7	0.6	1.3	1.0	0.6	3.2	0.0	1.6	1.9	0.9	0.5	0.8	0.2	0.6	1.8	2.3	0.3
$C_{22:1}$	0.0	0.0	0.0	0.0	0.0	0.0	0.0	0.0	0.1	0.0	0.0	0.0	0.0	0.0	0.0	0.0	0.0	0.0	0.0	0.0	0.0	0.0	0.0	0.0	0.0	0.0	0.0	0.0	0.0	0.0
$C_{23:0}$	0.0	0.0	0.0	0.0	0.0	0.0	0.3	0.0	0.0	0.0	0.0	0.0	0.1	0.0	0.0	0.0	0.0	0.0	0.0	0.0	0.0	0.0	0.0	0.0	0.0	0.0	0.0	0.0	0.0	0.0
$C_{24:0}$	1.1	0.1	0.4	0.3	1.3	0.1	0.9	0.1	0.0	0.2	0.4	0.4	0.3	0.3	0.2	0.1	0.3	0.1	1.0	0.5	0.3	0.6	0.2	0.2	0.3	0.1	0.1	0.5	0.4	0.1
$C_{26:0}$	0.0	0.0	0.0	0.0	0.0	0.0	0.2	0.0	0.0	0.0	0.0	0.0	0.0	0.0	0.0	0.0	0.0	0.0	0.0	0.0	0.0	0.0	0.0	0.0	0.0	0.0	0.0	0.0	0.0	0.0
% PUFA	15.5	2.3	4.9	7.1	13.2	1.3	7.8	1.7	44.6	5.4	0.9	4.1	2.6	0.4	6.8	7.7	5.6	2.1	2.3	1.9	11.4	4.5	0.9	1.6	2.4	39.7	30.7	8.4	0.0	0.0
ω-hydroxy-$C_{16:0}$	1.0	0.3	1.1	1.3	0.4	0.1	0.4	0.4	15.8	1.3	0.1	0.4	0.1	0.1	0.4	0.2	0.2	1.3	0.2	0.5	0.3	0.3	0.1	0.3	0.4	0.8	0.4	0.5	2.7	0.6
ω-hydroxy-$C_{18:1\omega9}$	0.8	0.0	0.5	0.5	0.2	0.0	0.4	0.0	0.0	0.4	0.0	0.1	0.0	0.0	0.2	0.1	0.1	0.2	0.1	0.1	0.2	0.2	0.0	0.1	0.3	1.1	0.4	0.2	0.7	0.2
18.(8-11)-dihydroxy-	5.0	1.0	9.3	7.2	1.5	0.2	2.3	1.9	7.8	7.2	0.1	2.9	0.9	0.2	1.1	0.6	0.8	3.0	1.7	3.7	2.3	1.9	0.0	1.3	2.5	2.5	2.5	1.7	3.1	0.9
ω-$C_{16:0}$ diacid	0.3	0.0	0.3	0.2	0.0	0.0	0.1	0.0	0.0	0.2	0.0	0.1	0.0	0.0	0.0	0.0	0.0	0.0	0.1	0.1	0.0	0.1	0.0	0.0	0.1	0.0	0.0	0.0	0.1	0.0
ω-hydroxy-$C_{22:0}$	92.9	98.6	88.8	90.8	97.9	99.7	96.9	97.6	76.4	91.0	99.8	96.5	98.9	99.7	98.3	99.1	98.8	95.5	97.9	95.6	97.2	97.5	99.9	98.3	96.7	95.6	96.6	97.5	93.5	98.3

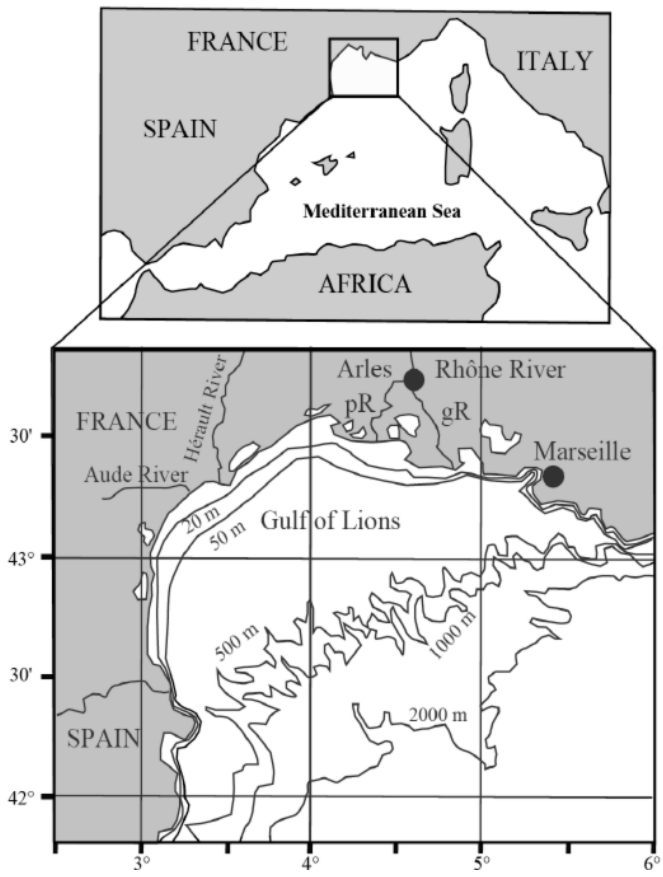

Figure 1. Rhone River mouth area and sampling location: “Arles”. gR and pR mean grand Rhone and petit Rhone which are the two arms of the river.

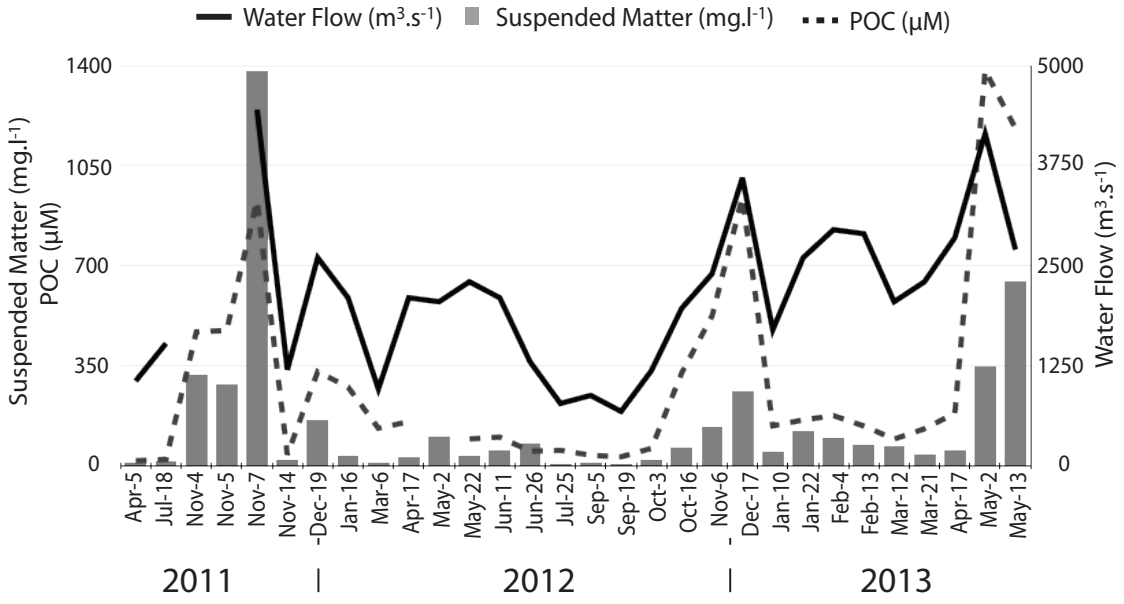

Figure 2: Water Flow ($m^3.s^{-1}$), Suspended Particulate Matter ($mg.l^{-1}$) and Particulate Organic Carbon (POC, µM) of Rhone waters on our sampling dates (MOOSE data). Samples span a wide range of water flow conditions.

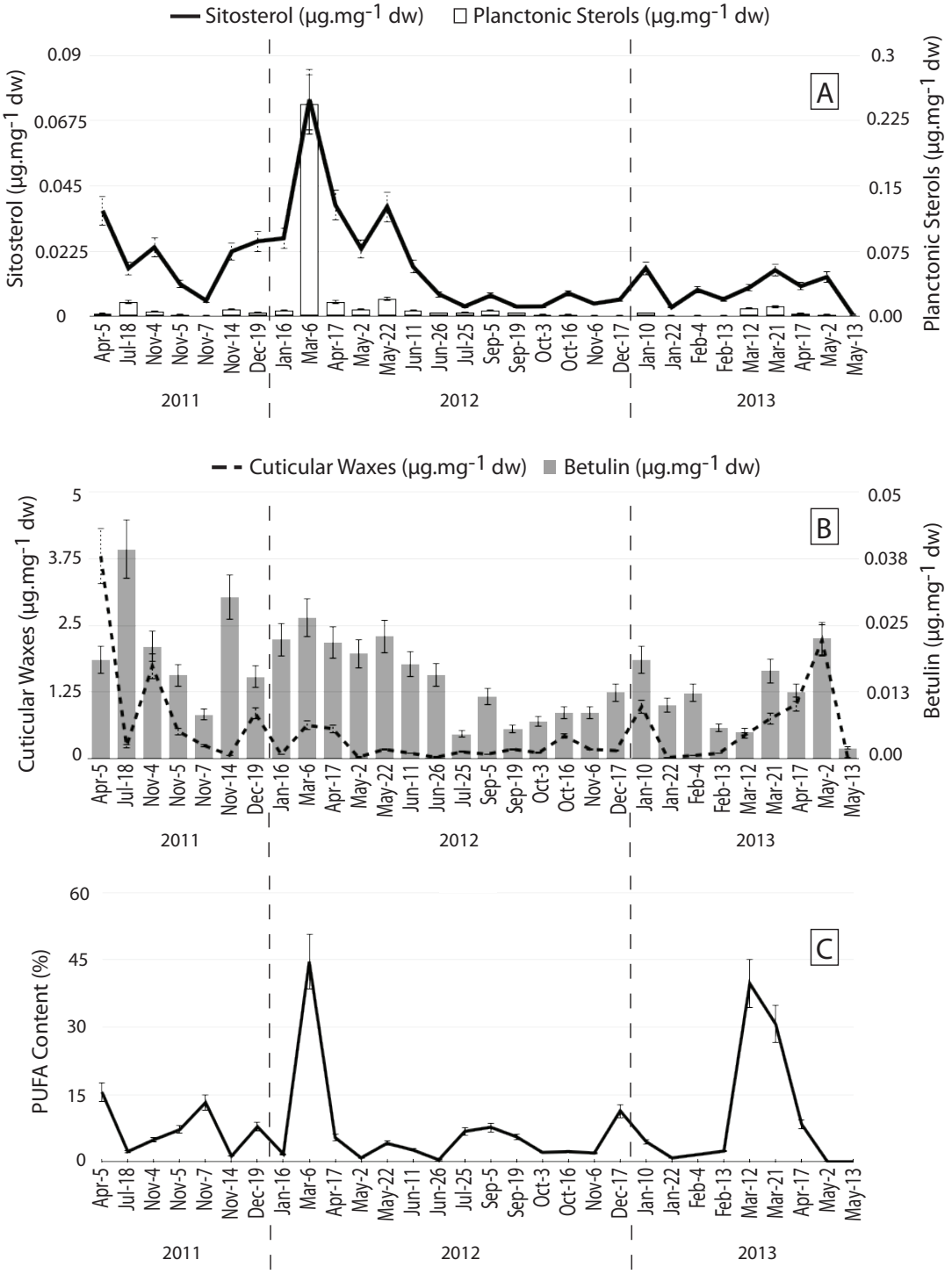

Figure 3: Sitosterol and planktonic sterols (A), cuticular waxes and betulin (B), and Poly-Unsaturated Fatty Acid (PUFA) (C) contents of the different samples. Standard error shown was estimated to be 14% (see section 2.3). Phytoplanktonic blooms are evidenced by the spike in planktonic sterols, and while the other tracers show the terrigenous origin of the POM sampled, the ubiquitous nature of sitosterol is made clear.

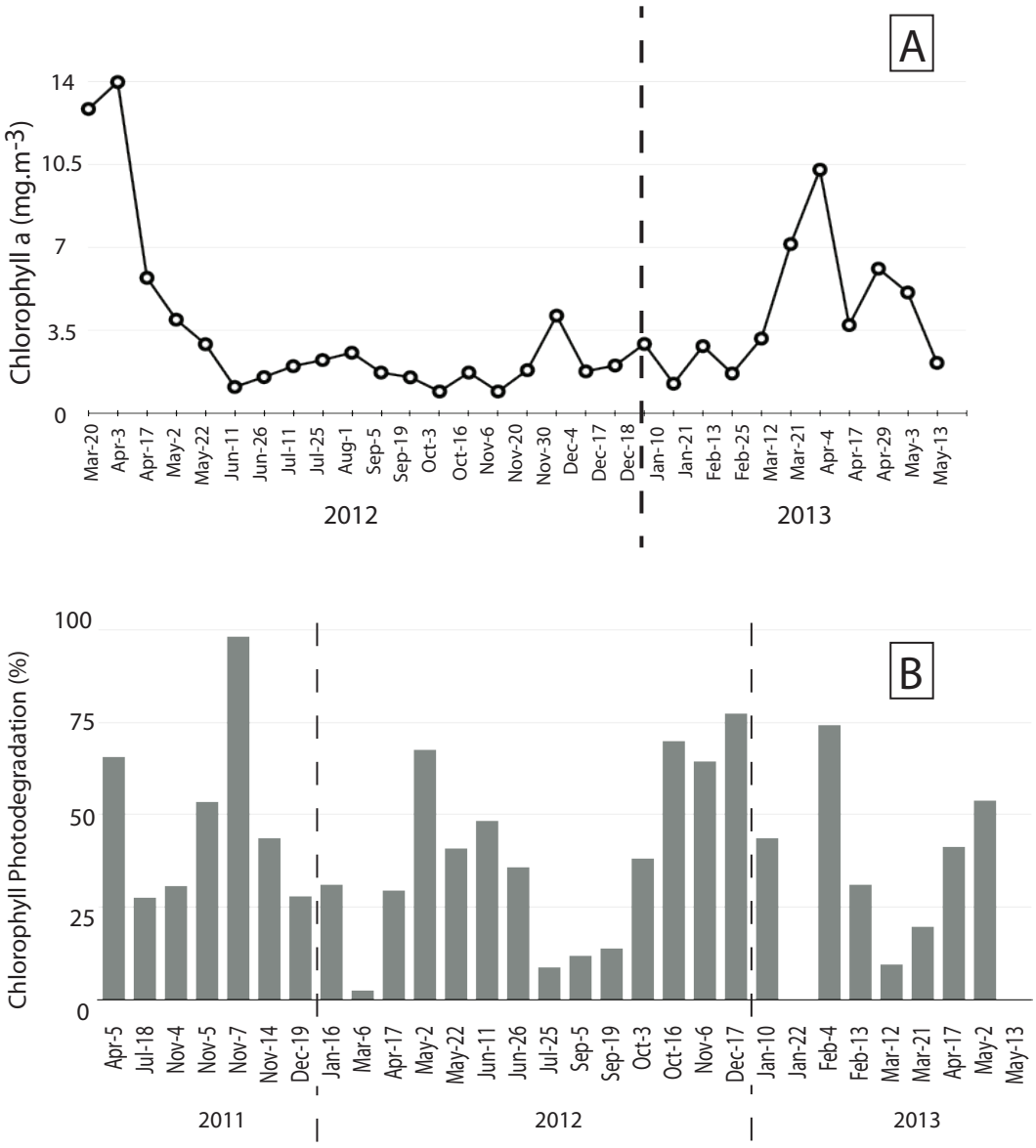

Figure 4: Chlorophyll a levels (MOOSE data) and percentage of photodegradation of chlorophyll (calculated using CPPI (Cuny et al., 1999) in the Rhone waters on and around sample dates

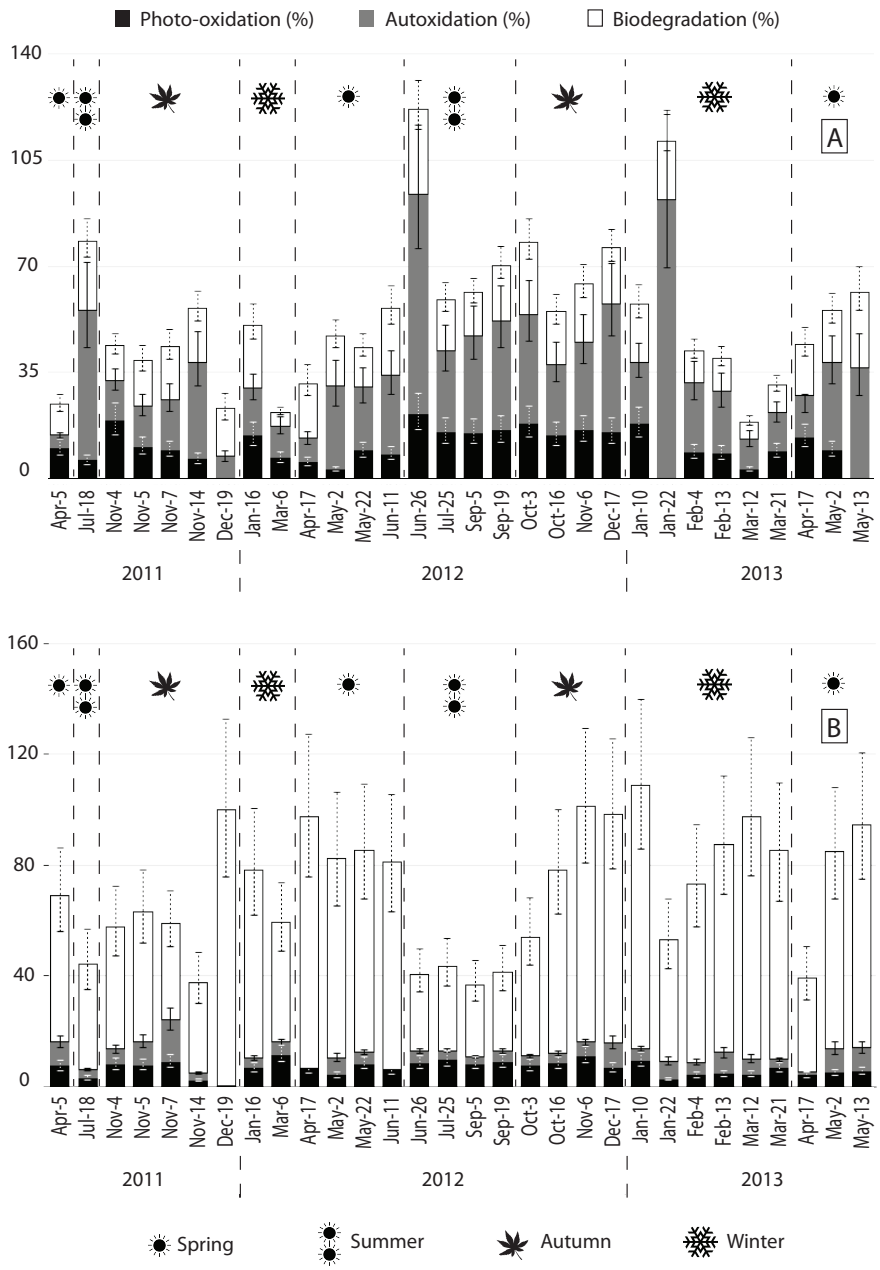

Figure 5: Biotic and abiotic degradation of sitosterol (A) and cholesterol (B) in the different samples. Full error shown here incorporates the 14% analytical standard error estimated for lipid quantification for all terms of the equations used. Sitosterol and cholesterol clearly have very different degradation patterns.

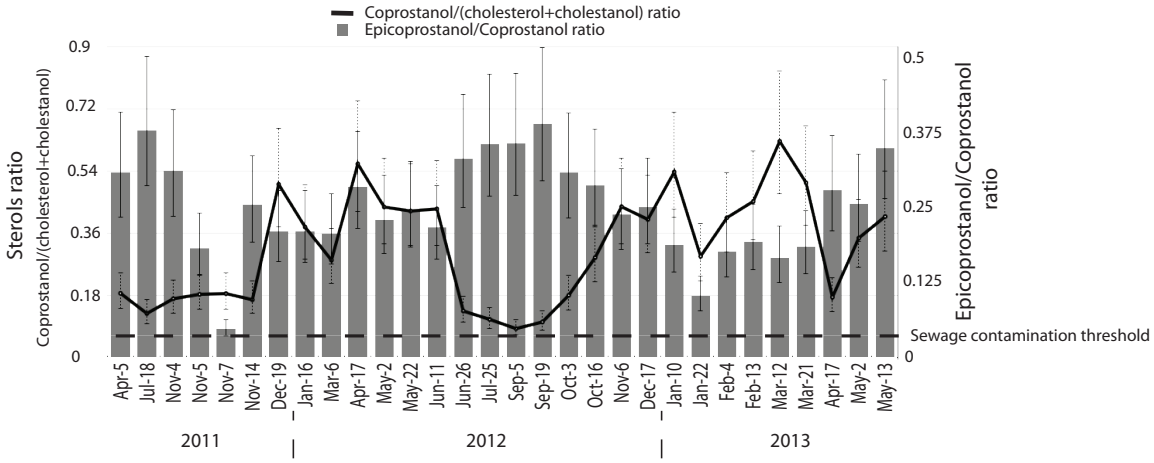

Figure 6: Coprostanol:(cholesterol+cholestanol) and epicoprostanol:coprostanol ratios of the different samples. Full error shown here incorporates the 14% analytical standard error estimated for lipid quantification for all terms of the ratios. Contamination threshold is 0.06 (See section 3.3.2).

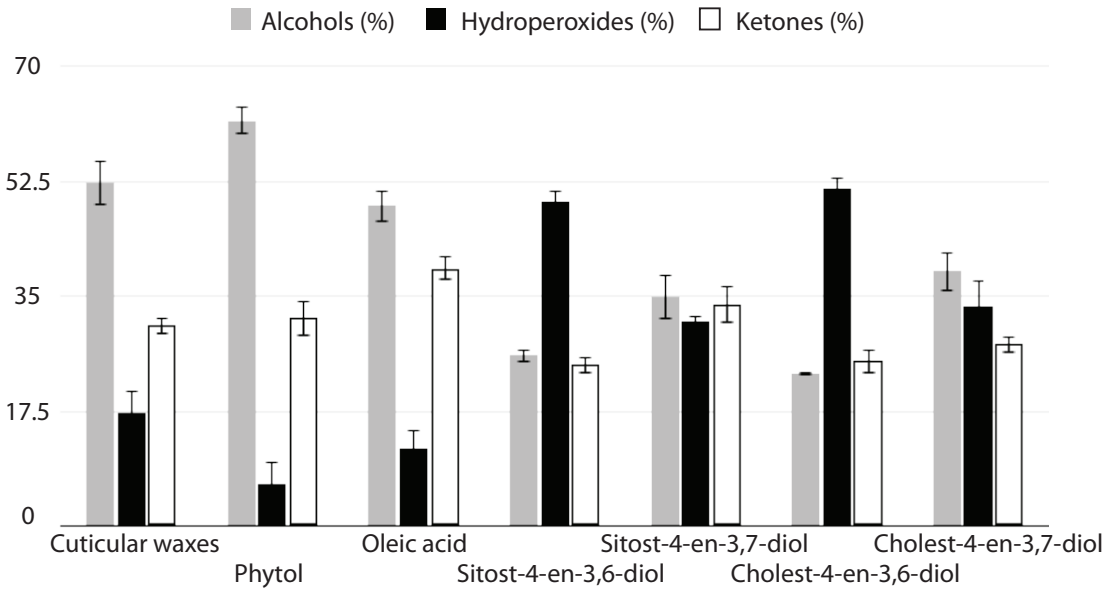

Figure 7: Relative percentages of intact hydroperoxides and their ketonic and alcoholic degradation products measured in the case of w-hydroxyoleic (cuticular waxes) and oleic acids, phytol, sitosterol and cholesterol oxidation products. Standard error was calculated based on the results obtained for all samples.